Time-Dependent DNA Condensation Induced by Amyloid β-Peptide

Haijia Yu, Jinsong Ren, and Xiaogang Qu
Division of Biological Inorganic Chemistry, Key Laboratory of Rare Earth Chemistry and Physics, Changchun Institute of Applied Chemistry, Graduate School of the Chinese Academy of Sciences, Changchun, Jilin, China

ABSTRACT The major protein component of the amyloid deposition in Alzheimer's disease is a 39–43 residue peptide, amyloid β (Aβ). Aβ is toxic to neurons, although the mechanism of neurodegeneration is uncertain. Evidence exists for non-B DNA conformation in the hippocampus of Alzheimer's disease brains, and Aβ was reportedly able to transform DNA conformation in vitro. In this study, we found that DNA conformation was altered in the presence of Aβ, and Aβ induced DNA condensation in a time-dependent manner. Furthermore, Aβ sheets, serving as condensation nuclei, were crucial for DNA condensation, and Cu^{2+} and Zn^{2+} ions inhibited Aβ sheet-induced DNA condensation. Our results suggest DNA condensation as a mechanism of Aβ toxicity.

INTRODUCTION

Amyloid β (Aβ) is a 39–43 amino acid polypeptide that is proteolytically derived from the transmembrane amyloid precursor protein (1–3). Aβ is the main component of neuritic plaques in the brains of Alzheimer's disease (AD) patients (4). Aβ40 is the predominant peptide species at the heterogeneous carboxyl terminus (5,6).

AD is a neurodegenerative disorder of complex origin. The mechanism of Aβ neurotoxicity is controversial. Previous studies found that intracellular aggregates of Aβ were toxic and that neurotoxicity was related to the degree of Aβ aggregation (7–9). Furthermore, it was recently reported that soluble oligomeric species of Aβ were more toxic than nonsoluble species (10,11).

Aβ aggregate formation is influenced by various experimental conditions (12–14), including pH, ionic strength, metal ions, membrane-like surface, incubation time, temperature, and hydration forces. In vitro studies (15–17) have demonstrated that low concentrations of Aβ induce neuronal apoptosis with DNA condensation, and using fluorescence microscopy, DNA condensation was observed in cells treated with Aβ (15,17). Furthermore, studies of DNA conformation in the hippocampus of AD brains (18) showed Z-DNA conformation, and supercoiled DNA treated with Aβ was more compact and condensed than nontreated DNA (19). However, the mechanism of condensation is obscure. DNA condensation is important in the cell cycle. It is involved in many biological processes, including gene expression (20) and chromosomal changes (21), and it is crucial for successful gene therapy. Thus, examining interactions of Aβ and DNA will be helpful for understanding Aβ neurotoxicity.

Aβ undergoes a time-dependent structural transition (13,22) from random coil to β-sheet in aqueous solutions, and this transition is thought to be related to its neurotoxicity. In this study, we studied the interactions between Aβ and DNA using circular dichroism, fluorescence spectroscopy, a replacement binding assay, electrophoresis, atomic force microscopy (AFM), and metal ion inhibition. We found that low concentrations of Aβ induced DNA condensation in a time-dependent manner. Additionally, Aβ-sheets, serving as condensation nuclei, were crucial for DNA condensation, and both Cu^{2+} and Zn^{2+} ions inhibited Aβ sheet-induced DNA condensation.

MATERIALS AND METHODS

Peptide

Aβ40 (lot No. 091K49551) and Aβ1–12 (lot No. 122K1377) were purchased from Sigma (St. Louis, MO). The peptide was first dissolved in 1,1,1,3,3,3-hexafluoro-2-propanol (HFIP) at the concentration of 1 mg/ml. The solution was shaking at 4°C for 2 h in a sealed vial for further dissolution and was then stored at −20°C as a stock solution (22). Before use, the solvent HFIP was removed by evaporation under a gentle stream of nitrogen and peptide was dissolved in 20 mM Tris buffer, pH 7.4.

Reagents

PolydGdC:polydGdC was a product of Pharmacia (Uppsala, Sweden, lot No. 2087910021) and calf thymus DNA was purchased from Sigma and purified as described earlier (23). HFIP was obtained from Acros Organics (Geel, Belgium). Ethidium bromide (EB) was purchased from USB (Cleveland, OH). (3-Aminopropyl) triethoxysilane (APTES) was purchased from Aldrich (St. Louis, MO). Solutions were all prepared in ultrapure water purified through a Milli-Q system (Millipore, Billerica, MA).

Circular dichroism measurements

Circular dichroism (CD) spectra of polydGdC:polydGdC with Aβ40 at different incubation time were measured from 200 nm to 380 nm on a JASCO (Tokyo, Japan) J-810 spectropolarimeter with a computer-controlled water bath (24,25). The optical chamber of CD spectrometer was deoxygenated with dry purified nitrogen (99.99%) for 45 min before use and kept the

Submitted July 17, 2006, and accepted for publication September 14, 2006.

Address reprint requests to Xiaogang Qu, Division of Biological Inorganic Chemistry, Key Laboratory of Rare Earth Chemistry and Physics, Changchun Institute of Applied Chemistry, Chinese Academy of Sciences, Changchun, Jilin 130022, China. Tel.: 86-431-526-2656; Fax: 86-431-5262656; E-mail: xqu@ciac.jl.cn.

0006-3495/07/01/185/07 $2.00

doi: 10.1529/biophysj.106.093559

nitrogen atmosphere during experiments. Three scans were accumulated and automatically averaged.

Ethidium bromide displacement and light scattering measurements

We used EB as a fluorescent probe to characterize DNA condensation because EB would be excluded out of their DNA binding sites when DNA condensed and its fluorescence would become comparable to that of free EB molecules (23). Fluorescence measurements were carried out on a JASCO FP-6500 spectrofluorometer at 20°C (25). Fluorescence spectra were monitored at different incubation time. The EB emission signal at 585 nm was translated as a relative value as $(F\text{-}F_0)/(F_{max}\text{-}F_0)$, where F_0 and F_{max} are the EB fluorescence intensity of free and bound with DNA.

The DNA condensation was monitored by light scattering on a JASCO FP-6500 spectrofluorimeter. The increasing intensity of light scattered at 90° from the incident beam was measured at 330 nm along with the increased incubation time.

UV-Vis absorption measurements

Absorbance measurements and melting experiments were made on a Cary 300 (Varian, Palo Alto, CA) UV/Vis spectrophotometer, equipped with a Peltier temperature control accessory (23,24). All UV/Vis spectra were measured from 190 nm and 340 nm in 1.0 cm-path length cell.

An AFM (Nanoscope IIIa, Digital Instruments, Santa Barbara, CA) was used to image polydGdC:polydGdC in the presence or absence of Aβ peptide at different incubation time. The sample solution was deposited onto a piece of freshly cleaved mica and rinsed with water and dried before measurements (23). Tapping mode was used to acquire the images under ambient condition.

Gel retarded assay

DNA and DNA/Aβ40 samples were prepared at room temperature with different incubation time. The samples were then loaded on 0.8% agarose electrophoresis (with TAE buffer) at 8 V/cm during the room temperature for 30 min. After EB stained DNA was visualized and photographed (25).

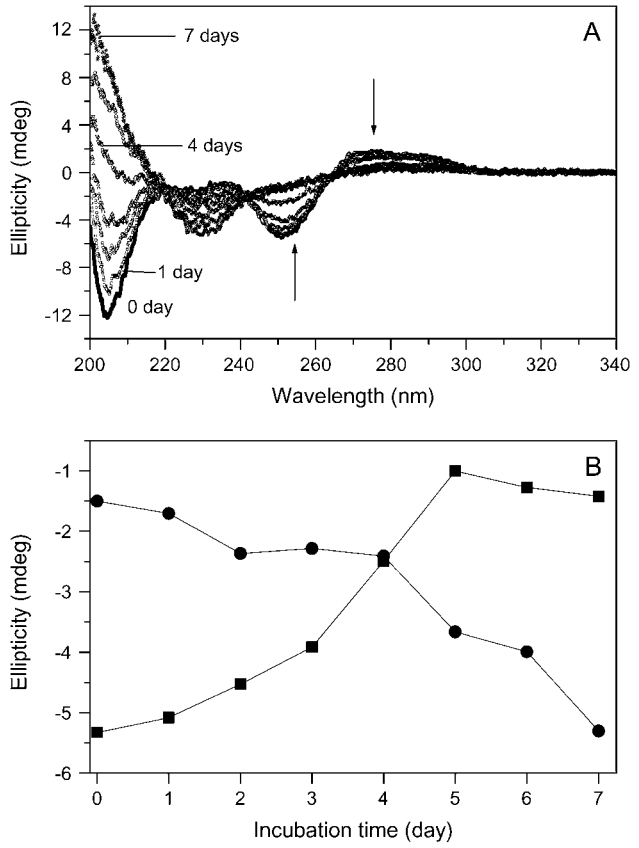

FIGURE 1 Circular dichroism spectral changes of polydGdC:polydGdC induced by incubation with Aβ40. (*A*) DNA in the presence of Aβ measured at different incubation time. 0 day (*solid line*); 1 day (*squares*); 2 days (*circles*); 3 days (*uppward triangles*); 4 days (*downward triangles*); 5 days (*diamonds*); 6 days (*crosses*); and 7 days (*stars*). [DNA] = 15 μM; [Aβ] = 1 μM; Aβ signal was subtracted respectively. (*B*) Plot of CD intensity at the 250 nm (*squares*) or at 230 nm (*circles*) as a function of the incubation time. The data were adopted from Fig. 1 *A*. Experimental details as described in the Materials and Methods section.

RESULTS AND DISCUSSION

To determine whether Aβ influences DNA conformation, we measured CD spectra of polydGdC:polydGdC in the absence and presence of Aβ. Fig. 1 *A* showed B-form DNA with two typical bands at 250 nm and 272 nm in the absence of Aβ. In accordance with previous results (26) there was no immediate change in CD intensity when Aβ was added. However, the 250 nm and 272 nm bands diminished with longer incubation time at room temperature. During the initial 1–2 day incubation, the CD intensity decreased slowly and then more rapidly as incubation continued (Fig. 1 *B*). Ultimately, the bands nearly disappeared, and a 230 nm negative CD band appeared. A 205-nm band, which is indicative of DNA structure, changed from negative to positive. Together, the changes indicate that there was a DNA conformational transition during incubation with Aβ and that the secondary structure of DNA was disturbed.

Gel retardation has been widely used to monitor DNA structural change (27), and we used gel electrophoresis to examine conformational changes in DNA during incubation with Aβ. The electrophoresis image (Fig. 2) and CD spectral

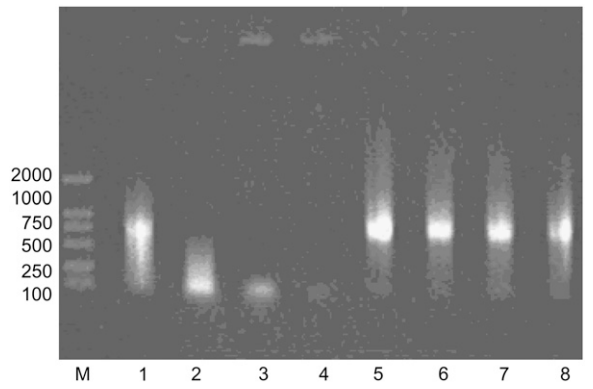

FIGURE 2 Effect of Aβ40 fragment on mobility of DNA in 0.8% agarose gel electrophoresis stained by EB. Lane M was the DNA marker. Lanes 1–4 were the samples of polydGdC:polydGdC with Aβ incubated at room temperature for 1, 2, 3, and 4 days, respectively. As control, lanes 5–8 were polydGdC:polydGdC alone incubated for 1, 2, 3, and 4 days, respectively.

analysis show that DNA underwent condensation. Initially, DNA was more compact, which may indicate a first-step condensate with a faster mobility than that of the 100 bp marker DNA, as previously reported (27). However, the quantum of that DNA form decreased over time (Fig. 2, *lanes 3* and *4*). Furthermore, DNA was present in the wells of the gel, which might represent complete condensation of DNA. There were no conformational changes in DNA that was incubated without Aβ (Fig. 2, *lanes 5–8*).

Compact DNA is resistant to intercalating dyes (28–31), and several DNA intercalators such as ToTo (28), YoYo (29), ethidium bromide (EB) (30), and syber Gold (31), have been used as fluorescent probes for DNA condensation. Here, we used an EB fluorescence quenching assay to examine DNA condensation. Fig. 3 *A* shows EB fluorescence measured at different incubation times. In DNA samples that were incubated with Aβ, EB intensity decreased, indicating that EB was excluded from binding sites. After 1 week, EB intensity was comparable to that of free equimolar EB. In contrast, there was very little change in EB intensity in DNA samples that were incubated without Aβ, even after 10 days. This observation indicates that Aβ induced DNA condensation, and it is consistent with the CD and gel electrophoresis results. In addition to polydGdC:polydGdC, we examined calf thymus DNA, which is a natural double-stranded DNA. We found that Aβ also induced calf thymus DNA condensation in a time-dependent manner (data not shown). These results indicate that Aβ can cause not only specific polydGdC:polydGdC DNA condensed but also natural DNA showing these phenomena more general. Further studies using different types of DNA are undergoing in our laboratory.

Aβ-induced DNA condensation was further demonstrated by light scattering (32). Fig. 3 *C* shows that DNA and Aβ formed aggregates in solution that scattered light. Monitoring the 90° light scattering intensity as a function of incubation time showed that the formation of DNA/Aβ aggregates was slow, as suggested by the EB replacement data.

Fig. 4 shows changes in DNA absorption at 260 nm. After incubation with Aβ, absorption decreased, and the band had a red shift from 260 nm to 270 nm. The decrease in absorption at 260 nm and the corresponding increase in scattering at 320 nm imply the formation of condensates (33). DNA UV spectral changes also suggest that DNA was condensed in the presence of Aβ.

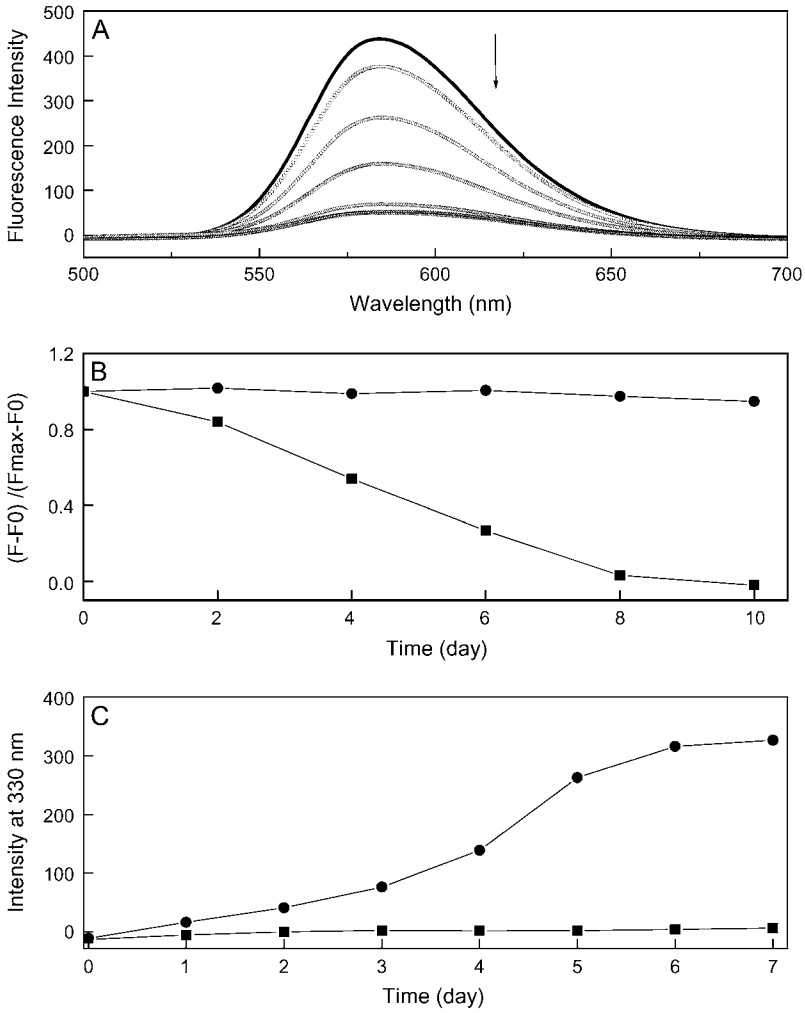

FIGURE 3 (*A*) Fluorescence spectra of EB when bound to polydGdC:polydGdC in the presence of Aβ. EB fluorescence was decreased with increasing the incubation time. (*B*) Normalized EB fluorescence at 585 nm as a function of incubation time in the presence (*solid squares*) or absence (*solid circles*) of Aβ. (*C*) Plot of light scattering intensity at 330 nm as a function of 1 μM Aβ incubated with 15 μM DNA (*solid circles*); 1 μM Aβ alone (*solid squares*). All incubations were done at room temperature. Details as described in the Materials and Methods section.

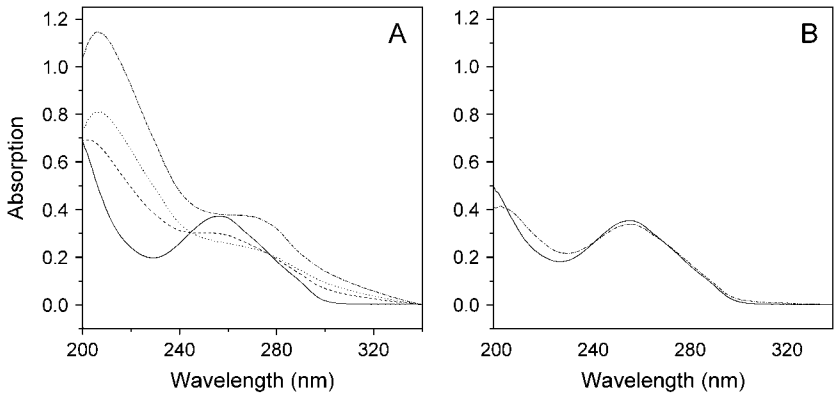

FIGURE 4 Absorption spectral changes of polydGdC:polydGdC incubated with Aβ peptide. (*A*) DNA incubated with Aβ; (*B*) DNA alone. The sample was incubated for 0 day (*solid lines*), 3 days (*dash lines*), 5 days (*dot lines*), and 7 days (*dash-dot lines*), respectively.

AFM was used to characterize DNA condensation and structure. After 5-day incubation, DNA/Aβ condensates were formed (Fig. 5). A large number of DNA molecules were tangled together to form condensates (23). The condensates were primarily in the form of toroidals or globules, and the particle diameter ranged from 50–200 nm. This result is consistent with the electrophoresis and light scattering results.

DNA condensation was induced by the slow conformational transition of Aβ in solution. After Aβ was dissolved in buffer, it was in a random coil and did not immediately change to a β-sheet conformation. Instead, the transition to β-sheet occurred after several days of incubation at room temperature (Fig. 6), in agreement with previous reports (13,22). We assume that the β-sheet served as condensation nuclei to induce DNA condensation. For comparison, we incubated polydGdC:polydGdC with Aβ at 2°C, and did not observe any changes to DNA secondary structure (Fig. 7). This indicates that formation of β-sheets is important for DNA condensation, since low temperatures can destabilize hydrophobic interactions and inhibit the transition of Aβ to β-sheets (34). Another evidence to support β-sheet inducing DNA condensation was that Aβ1–12 could not make DNA condensation under the same conditions used for Aβ1–40. Gel electrophoresis showed that DNA was not condensed with incubation of Aβ1–12 (Fig. 8), and CD spectra (Fig. 9) indicated that Aβ1–12 did not change to a β-sheet conformation, in accordance with previous studies on Aβ1–13 (35), demonstrating that β-sheet conformation is crucial for inducing DNA condensation.

Aβ is a metalloprotein. Both Cu^{2+} and Zn^{2+} bind to Aβ and can prevent or delay the formation of fibrils with β-sheet conformation (22,36). We studied the effects of Cu^{2+} and Zn^{2+} on DNA/Aβ interactions. As shown in Fig. 10, both ions delayed Aβ-induced DNA condensation. The results provide indirect evidence that β-sheets are an active inducer of DNA condensation.

Prion protein is an amyloid-forming protein, and like AD, prion disease results from protein misfolding with a conformational transition from α-helix to β-sheet. Regarding the interaction of prion protein (or its fragment PrP106–126) and DNA, previous studies have shown that DNA promotes prion protein polymerization and induces time-dependent DNA condensation (37,38). This is in keeping with our conclusion that β-sheets induce time-dependent DNA condensation. It is known that α-helix and β-sheet structures of proteins interact with DNA. The β-sheet structure interacts favorably with DNA, and H-bonds may form between peptide NH groups and deoxyribose O-3′ atoms (39). According to this assumption, Aβ may be folded in a predominantly β-sheet secondary structure, which is promoted by the presence

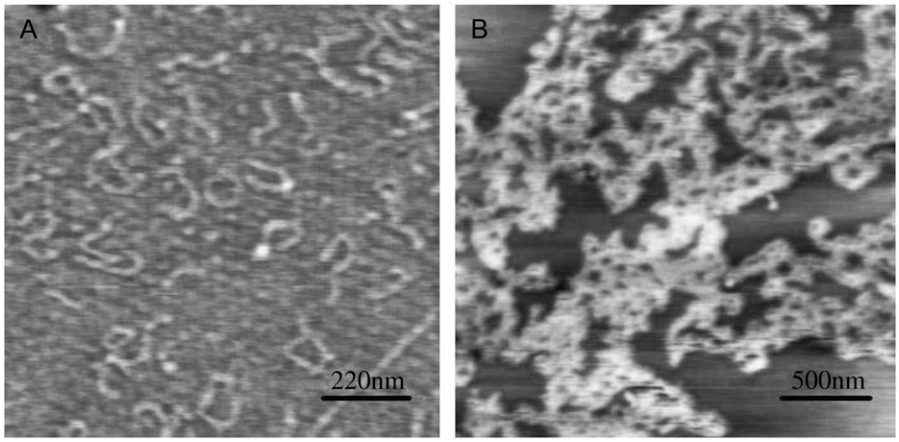

FIGURE 5 AFM images of DNA condensates induced by Aβ40. (*A*) polydGdC:polydGdC alone; (*B*) DNA with Aβ (the proportion is as same as that used in the spectral experiments). Incubation time, 5 days. Details as described in the Materials and Methods section.

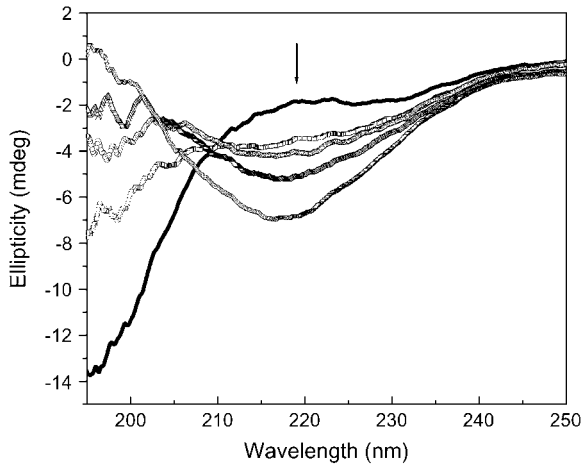

FIGURE 6 CD spectra of Aβ40 peptide (50 μM) after incubation at room temperature for different time. 0 day (*black line*); 1 day (*open squares*); 3 days (*open circles*); 5 days (*uppward triangles*); and 7 days (*downward triangles*). The spectral data showed that the relative amount of β-sheet conformation was increased with increasing the incubation time.

of DNA, and serve as a condensation nuclei, which increases its propensity to aggregate with DNA during incubation.

Aβ is the major constituent of senile plaques, and although the mechanisms that lead to Aβ accumulation are not clear, Aβ is involved in AD pathogenesis, and may be the predominant causative factor of AD (2). A link has been made between AD and nucleic acid through the identification of mRNA in senile plaques. As shown by acridine orange histochemistry, RNA is one of the nonproteinaceous components of neurofibrillary tangles and senile plaques (40,41). High affinity RNA aptamers against Aβ were isolated, and β-sheet conformation was thought to be the RNA binding form (42). Previous results indicate that intracellular accumulation of Aβ rather than extracellular deposition of Aβ

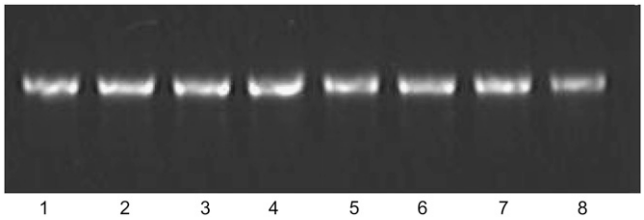

FIGURE 8 Effect of Aβ1–12 fragment on mobility of DNA in 0.8% agarose gel electrophoresis. Lanes 1–4 were the samples of polydGdC:polydGdC with Aβ1–12 incubated at room temperature for 1, 2, 3, and 4 days, respectively. As control, lanes 5–8 were polydGdC:polydGdC alone incubated for 1, 2, 3, and 4 days, respectively.

induce apoptosis (43, 44). Aβ localized in the nuclear region of AD cells (19) enable structural alteration of DNA.

Oxidative damage to DNA in AD brains may play a role in cell death (45). Previous studies have also shown changes in chromatin from a normal euchromatin structure to a condensed heterochromatin structure (46). Recently, rigid, non-B DNA conformations were observed in severely affected AD brains (18), and it was shown that Aβ can modulate helical properties of DNA, especially supercoiled DNA (19). Interactions among biomolecules are often modulated by their conformation. Aβ exists in several conformations (47), based on incubation time and temperature in vitro. Our results indicate that in the presence of Aβ, DNA was condensed and its structure was disturbed with increasing incubation time. DNA condensation can influence gene expression and transcription in AD cells. Previous studies (15–17) have shown that low concentrations of Aβ induced neuronal apoptosis with DNA condensation. Therefore, the interactions of Aβ and DNA are important and may have a role in the pathogenesis of AD (18,19,45,46), the mechanisms of which need further clarification.

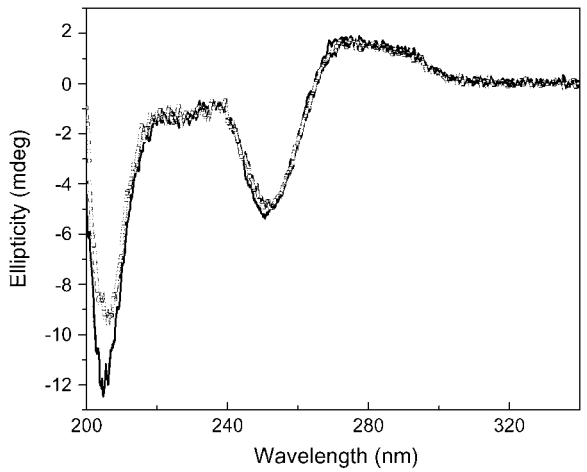

FIGURE 7 CD spectra of polydGdC:polydGdC with Aβ40 at 2°C before (*solid line*) or after incubated for 7 days (*open squares*). Details were described in the experimental section.

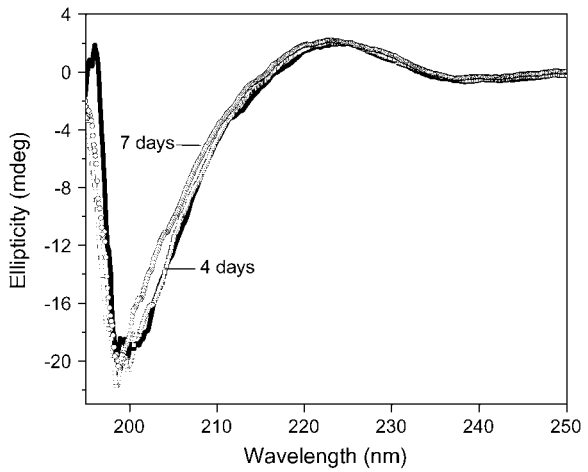

FIGURE 9 CD spectra of Aβ1–12 peptide (200 μM) after incubation at room temperature under the same conditions used for Aβ40. 0 day (*black line*); 4 days (*open squares*); and 7 days (*open circles*).

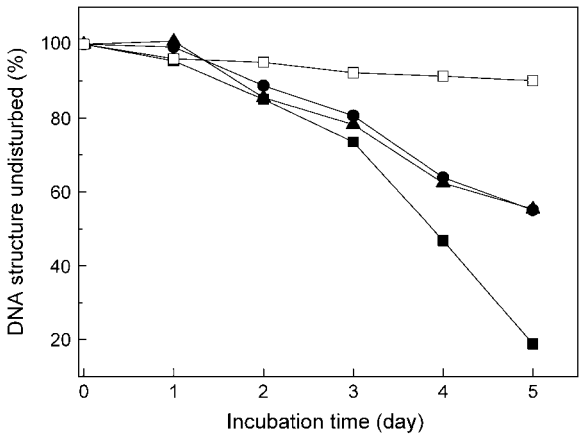

FIGURE 10 Inhibition effects of Cu^{2+} and Zn^{2+} on Aβ40 induced DNA condensation. 15 μM DNA was incubated with 1 μM Aβ40 in the presence or absence of 1 μM metal ions. Aβ signal was subtracted respectively; CD spectra were measured at different incubation time and the proportions of undisturbed DNA were determined using the ellipticity at 250 nm. DNA with Aβ40 (*solid squares*); DNA with Aβ40 in the presence of Cu^{2+} (*circles*); DNA with Aβ40 in the presence of Zn^{2+} (*upper triangles*); and DNA alone (*open squares*).

In summary, our results indicate that Aβ induces double-stranded DNA condensation in vitro, and the condensation is time-dependent, as examined with circular dichroism, fluorescence spectroscopy, a replacement binding assay, electrophoresis, AFM, and metal ion inhibition. β-sheets, serving as condensation nuclei, are crucial for inducing DNA condensation.

The authors are grateful for the referees' helpful comments on the manuscript.

This project was supported by the National Natural Science Foundation of China (20225102, 20331020, 20325101, 20473084), funds from Jilin Province and Hundred People Program from the Chinese Academy of Sciences.

REFERENCES

1. Masters, C. L., G. Simms, N. A. Weinman, G. Multhaup, B. L. McDonald, and K. Beyreuther. 1985. Amyloid plaque core protein in Alzheimer's disease and Down syndrome. *Proc. Natl. Acad. Sci. USA.* 82:4245–4249.
2. Selkoe, D. J. 1996. Amyloid β-protein and the genetics of Alzheimer's disease. *J. Biol. Chem.* 271:18295–18298.
3. Soto, C., and E. M. Castano. 1996. The conformation of Alzheimer's β peptide determines the rate of amyloid formation and its resistance to proteolysis. *Biochem. J.* 314:701–707.
4. Sisodia, S. S. 1992. β-Amyloid precursor protein cleavage by a membrane bound protease. *Proc. Natl. Acad. Sci. USA.* 89:6075–6079.
5. Mori, H., K. Takio, M. Ogawara, and D. J. Selkoe. 1992. Mass spectrometry of purified amyloid β protein in Alzheimer's disease. *J. Biol. Chem.* 267:17062–17086.
6. Selkoe, D. J. 2004. Cell biology of protein misfolding: The examples of Alzheimer's and Parkinson's diseases. *Nat. Cell Biol.* 6:1054–1061.
7. Pike, C. J., D. Burdick, A. J. Walencewicz, C. G. Glabe, and C. W. Cotman. 1993. Neurodegeneration induced by β-amyloid peptides in vitro: the role of peptide assembly state. *J. Neurosci.* 13:1676–l 687.
8. Pike, C. J., A. J. Walencewicz, J. Kosmoski, D. H. Cribbs, C. G. Glabe, and C. W. Cotman. 1995. Structure-activity analyses of β-amyloid peptides: contributions of the β25–35 region to aggregation and neurotoxicity. *J. Neurochem.* 64:253–265.
9. Lorenzo, A., and B. A. Yankner. 1994. β-Amyloid neurotoxicity requires fibril formation and is inhibited by Congo red. *Proc. Natl. Acad. Sci. USA.* 91:12243–122 47.
10. Lambert, M. P., A. K. Barlow, B. A. Chromy, C. Edwards, R. Freed, M. Liosatos, T. E. Morgan, I. Rozovsky, B. Trommer, K. L. Viola, P. Wals, C. Zhang, C. E. Finch, G. A. Krafft, and W. L. Klein. 1998. Diffusible, nonfibrillar ligands derived from Abeta1–42 are potent central nervous system neurotoxins. *Proc. Natl. Acad. Sci. USA.* 95: 6448–6453.
11. Kim, H. J., S. C. Chae, D. K. Lee, B. Chromy, S. C. Lee, Y. C. Park, W. L. Klein, G. A. Krafft, and S. T. Hong. 2003. Selective neuronal degeneration induced by soluble oligomeric amyloid beta protein. *FASEB J.* 17:118–120.
12. Hilbich, C., B. Kisters-Woike, J. Reed, C. L. Masters, and K. Beyreuther. 1991. Aggregation and secondary structure of synthetic amyloid βA4 peptides of Alzheimer's disease. *J. Mol. Biol.* 218: 149–163.
13. Bush, A. I., W. H. Pettingell, G. Multhaup, M. D. Paradis, J. P. Vonsattel, J. F. Gusella, K. Beyreuther, C. L. Masters, and R. E. Tanzi. Rapid induction of Alzheimer Aβ amyloid formation by zinc. *Science* 265:1464–1467.
14. Yang, D. S., C. M. Yip, T. H. Huang, A. Chakrabartty, and P. E. Fraser. 1994. Manipulating the Amyloid-β aggregation pathway with chemical chaperones. *J. Biol. Chem.* 274:32970–32974.
15. Zeng, H., Q. Chen, and B. Zhao. 2004. Genistein ameliorates β-amyloid peptide (25–35)-induced hippocampal neuronal apoptosis. *Free Radical Bio. Med.* 36:180–188.
16. Pillot, T., B. Drouet, S. Queille, C. Labeur, J. Vandekerckhove, M. Rosseneu, M. Pinçon-Raymond, and J. Chambaz. 1999. The nonfibrillar amyloid β-peptide induces apoptotic neuronal cell death: involvement of its C-terminal fusogenic domain. *J. Neurochem.* 73: 1626–1634.
17. Blanc, E. M., M. Toborek, R. J. Mark, B. Hennig, and M. P. Mattson. 1997. Amyloid β-peptide induces cell monolayer albumin permeability, impairs glucose transport, and induces apoptosis in vascular endothelial cells. *J. Neurochem.* 68:1870–1881.
18. Anitha, S., K. S. R. Jagannatha, K. S. Latha, and M. A. Viswamitra. 2002. First evidence to show the topological change of DNA from B-DNA to Z-DNA conformation in the hippocampus of Alzheimer's brain. *NeuroMol. Med.* 2:289–298.
19. Hegde, M. L., S. Anitha, and K. S. Latha. 2003. First evidence for helical transitions in supercoiled DNA by amyloid beta peptide(1–42) and aluminum-A new insight in understanding Alzheimer's disease. *J. Mol. Neurosci.* 22:19–31.
20. Childs, A. C., D. J. Mehta, and E. W. Gerner. 2003. Polyamine-dependent gene expression. *Cell. Mol. Life Sci.* 60:1394–1406.
21. Arents, G., and E. N. Moudrianakis. 1993. Topography of the histone octamer surface: repeating structural motifs utilized in the docking of nucleosomal DNA. *Proc. Natl. Acad. Sci. USA.* 90:10489–10493.
22. Yoshiike, Y., K. Tanemura, O. Murayama, T. Akagi, M. Murayama, S. Sato, X. Sun, N. Tanaka, and A. Takashima. 2001. New insights on how metals disrupt amyloid β-aggregation and their effects on amyloid-β cytotoxicity. *J. Biol. Chem.* 276:32293–32299.
23. Li, X., Y. Peng, and X. Qu. 2006. Carbon nanotubes selective destabilization of duplex and triplex DNA and inducing B-A transition in solution. *Nucleic Acids Res.* 34:3670–3676.
24. Zhang, H., H. Yu, J. Ren, and X. Qu. 2006. PolydA and polyrA self-structured by A auropium and amino acid complex. *FEBS Lett.* 580: 3726–3730.
25. Zhang, H., H. Yu, J. Ren, and X. Qu. 2006. Reversible B/Z-DNA transition under the low salt condition and non-B-form PolydApolydT selectivity by a cubane-like Europium-L-aspartic acid complex. *Biophys. J.* 90:3203–3207.

26. Anitha, S., and K. S. R. Jagannatha. 2003. Challenges and excitements in understanding of abeta peptides and aluminium induce helical transitions in supercoiled DNA and POL. *J. Neurochem.* 87:93–93 (Suppl.).

27. Chittimalla, C., L. Zammut-Italiano, G. Zuber, and J. P. Behr. 2005. Monomolecular DNA nanoparticles for intravenous Delivery of genes. *J. Am. Chem. Soc.* 127:11436–11441.

28. Trubetskoy, V. S., V. G. Budker, L. J. Hanson, P. M. Slattum, J. A. Wolff, and J. E. Hagstrom. 1998. Self- assembly of DNA–polymer complexes using template polymerization. *Nucleic Acids Res.* 26:4178–4185.

29. Krishnamoorthy, G., G. Duportail, and Y. Mély. 2002. Structure and dynamics of condensed DNA probed by 1,1'-(4,4,8,8-Tetramethyl-4,8-diazaundecamethylene)bis[4-[[3-methylbenz- 1,3-oxazol- 2-yl]methylidine]-1,4-dihydroquinolinium] tetraiodide fluorescence. *Biochemistry.* 41:15277–15287.

30. Xu, Y. H., and F. C. Szoka. 1996. Mechanism of DNA release from cationic liposome/DNA complexes used in cell transfection. *Biochemistry.* 35:5616–5623.

31. McKenzie, D. L., K. Y. Kwok, and K. G. Rice. 2000. A potent new class of reductively activated peptide gene delivery agents. *J. Biol. Chem.* 275:9970–9977.

32. Thual, C., A. A. Komar, L. Bousset, E. Fernandez-Bellot, C. Cullin, and R. Melki. Structural characterization of *Saccharomyces cerevisiae* prion-like protein Ure2. *J. Biol. Chem.* 274:13666–13614.

33. Roy, K. B., T. Antony, A. Saxena, and H. B. Bohidar. 1999. Ethanol-induced condensation of calf thymus DNA studied by laser light scattering. *J. Phys. Chem. B.* 103:5117–5121.

34. De Felice, F. G., J. C. Houzel, J. Garcia-Abreu, P. R. F. Louzada, R. C. Afonso, M. N. L. Meirelles, R. Lent, V. M. Neto, and S. T. Ferreira. 2001. Inhibition of Alzheimer's disease b-amyloid aggregation, neurotoxicity, and in vivo deposition by nitrophenols: implications for Alzheimer's therapy. *FASEB J.* 15:1297–1299.

35. Bodles, A. M., D. J. S. Guthrie, P. Harriott, P. Campbell, and G. B. Irvine. 2000. Toxicity of non-Ab component of Alzheimer's disease amyloid, and N-terminal fragments thereof, correlates to formation of b-sheet structure and fibrils. *Eur. J. Biochem.* 267:2186–2194.

36. Zou, J., K. Kaijita, and N. Sugimoto. 2001. Cu^{2+} inhibits the aggregation of amyloid β-peptide(1–42) in vitro. *Angew. Chem. Int. Ed. Engl.* 40:2274–2277.

37. Nandi, P. K., and E. Leclerc. 1999. Polymerization of murine recombinant prion protein in nucleic acid solution. *Arch. Virol.* 144: 1751–1763.

38. Nandi, P. K., and P. Y. Sizaret. 2001. Murine recombinant prion protein induces ordered aggregation of linear nucleic acids to condensed globular structures. *Arch. Virol.* 146:327–345.

39. Church, G. M., J. L. Sussman, and S. Kim. 1977. Secondary structural complementarity between DNA and proteins. *Proc. Natl. Acad. Sci. USA.* 74:1458–1462.

40. Ginsberg, S. D., P. B. Crino, S. E. Hemby, J. A. Weingarten, V. M. Lee, J. M. Eberwine, and J. Q. Trojanowski. 1999. Predominance of neuronal mRNAs in individual Alzheimer's disease senile plaques. *Ann. Neurol.* 45:174–181.

41. Ginsberg, S. D., J. E. Galvin, T. Chiu, V. M. Lee, E. Masliah, and J. Q. Trojanowski. 1998. RNA sequestration to pathological lesions of neurodegenerative diseases. *Acta Neuropathol. (Berl.).* 96: 487–494.

42. Ylera, F., R. Lurz, V. A. Erdmann, and J. P. Furste. 2002. Selection of RNA aptamers to the Alzheimer's disease amyloid peptide. *Biochem. Biophys. Res. Commun.* 290:1583–1588.

43. Kienlen-Campard, P., S. Miolet, B. Tasiaux, and J. N. Octave. 2002. Intracellular amyloid-β1–42, but not extracellular soluble amyloid-β peptides, induces neuronal apoptosis. *J. Biol. Chem.* 277:15666–15670.

44. Gouras, G. K., J. Tsai, J. Naslund, B. Vincent, M. Edgar, F. Checler, J. P. Greenfield, V. Haroutunian, J. D. Buxbaum, H. Xu, P. Greengard, and N. R. Relkin. 2000. Intraneuronal Aβ42 accumulation in human brain. *Am. J. Pathol.* 156:15–20.

45. Lyras, L., N. J. Cairns, A. Jenner, P. Jenner, and B. Halliwell. 1997. An assessment of oxidative damage to proteins, lipids, and DNA in brain from patients with Alzheimer's disease. *J. Neurochem.* 68: 2061–2069.

46. Crapper, D. R., S. Quittkat, and U. De. Boni. 1979. Altered chromatin conformation in Alzheimer's disease. *Brain.* 102:483–495.

47. Golabek, A. A., C. Soto, T. Vogel, and T. Wisniewski. 1996. The interaction between Apolipoprotein E and Alzheimer's amyloid β-peptide is dependent on β-peptide conformation. *J. Biol. Chem.* 271:10602–10606.